

AD-A181 502

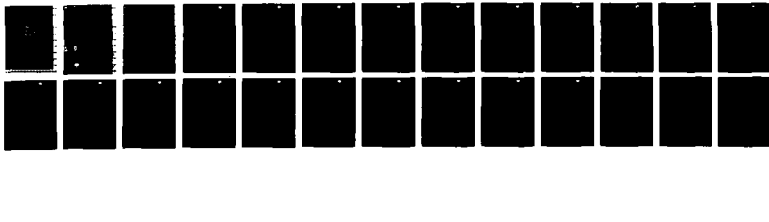
OHMIC CONTRACTS TO GALLIUM ALUMINUM ARSENIDE FOR HIGH  
TEMPERATURE APPLICA. (U) ROCKWELL INTERNATIONAL  
THOUSAND OAKS CA SCIENCE CENTER R W GRANT ET AL.  
APR 87 SC5485. AR AFOSR-TR-87-0719

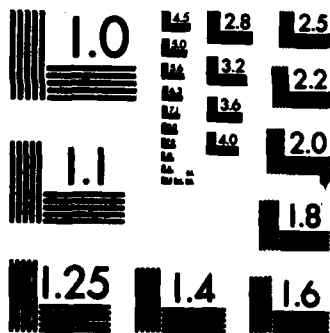
1/1

UNCLASSIFIED

F/G 9/1

NL





MICROCOPY RESOLUTION TEST CHART  
NATIONAL BUREAU OF STANDARDS-1963-A

SC5485.AR

SC5485.AR

Copy No. 4

# OHMIC CONTACTS TO GALLIUM ALUMINUM ARSENIDE FOR HIGH TEMPERATURE APPLICATIONS

AD-A181 502

ANNUAL TECHNICAL REPORT FOR THE PERIOD  
July 01, 1985 through June 30, 1986

CONTRACT NO. F49620-85-C-0120

Approved for public release;  
distribution unlimited.

Prepared for

Air Force Office of Scientific Research  
Directorate of Electronic and Material Sciences  
Bldg. 410  
• Bolling AFB, DC 20332-6448

R.W. Grant and J.R. Waldrop  
Principal Investigators

APRIL 1987

"The views and conclusions contained in this document are those of the authors and should not be interpreted as necessarily representing the official policies or endorsements, either expressed or implied, of the Air Force Office of Scientific Research or the U.S. Government."

Approved for public release; distribution unlimited



Rockwell International  
Science Center

AIR FORCE OFFICE OF SCIENTIFIC RESEARCH  
DIRECTORATE OF ELECTRONIC AND MATERIAL SCIENCES  
BOLLING AIR FORCE BASE, WASHINGTON, D.C. 20332-6448  
Approved for public release; distribution unlimited.  
MATTIE J. WOOD  
Chief, Technical Information Services

DTIC  
ELECTE  
JUN 15 1987  
S D

UNCLASSIFIED

SECURITY CLASSIFICATION OF THIS PAGE

## REPORT DOCUMENTATION PAGE

1a. REPORT SECURITY CLASSIFICATION <b>UNCLASSIFIED</b>		1b. RESTRICTIVE MARKINGS	
2a. SECURITY CLASSIFICATION AUTHORITY		3. DISTRIBUTION/AVAILABILITY OF REPORT  Approved for public release; distribution unlimited	
2b. CLASSIFICATION/DOWNGRADING SCHEDULE			
4. PERFORMING ORGANIZATION REPORT NUMBER(S) <b>SC5485.AR</b>		5. MONITORING ORGANIZATION REPORT NUMBER(S) <b>AFOSR-TN- 87-0719</b>	
6a. NAME OF PERFORMING ORGANIZATION <b>ROCKWELL INTERNATIONAL Science Center</b>	6b. OFFICE SYMBOL (If Applicable)	7a. NAME OF MONITORING ORGANIZATION <b>AFOSR</b>	
6c. ADDRESS (City, State, and ZIP Code) <b>1049 Camino Dos Rios Thousand Oaks, CA 91360</b>		7b. ADDRESS (City, State and ZIP Code) <b>Bldg 410 Bolling AFB, DC 20332-6448</b>	
8a. NAME OF FUNDING/SPONSORING ORGANIZATION <b>Air Force Office of Scientific Research</b>	8b. OFFICE SYMBOL (If Applicable) <b>NE</b>	9. PROCUREMENT INSTRUMENT IDENTIFICATION NUMBER  <b>CONTRACT NO. F49620-85-C-0120</b>	
8c. ADDRESS (City, State and ZIP Code) <b>Directorate of Electronic and Material Sciences Bolling AFB, DC 20332-6448</b>		10. SOURCE OF FUNDING NOS.	
11. TITLE (Include Security Classification) <b>OHMIC CONTACTS TO GALLIUM ALUMINUM ARSENIDE FOR HIGH TEMPERATURE APPLICATIONS</b>		PROGRAM ELEMENT NO. <b>61102F</b>	PROJECT NO. <b>2306</b>
		TASK NO. <b>B1</b>	WORK UNIT NO.
12. PERSONAL AUTHOR(S) <b>Grant, R.W. and Waldrop, J.R.</b>			
13a. TYPE OF REPORT <b>Annual Technical Report</b>	13b. TIME COVERED FROM <b>07/01/85</b> TO <b>06/30/86</b>	14. DATE OF REPORT (Yr., Mo., Day) <b>1987, APRIL</b>	15. PAGE COUNT <b>20</b>
16. SUPPLEMENTARY NOTATION			
17. COSATI CODES		18. SUBJECT TERMS (Continue on reverse if necessary; and identify by block number)	
FIELD	GROUP	SUB GR.	
19. ABSTRACT (Continue on reverse if necessary and identify by block number)			
<p>A method of modifying the <math>\text{r-GaAs}(100)</math> interface Fermi level position (<math>E_F^I</math>) has been investigated. For tunnel ohmic contacts the contact resistance depends exponentially on the energy difference between the conduction band minimum and <math>E_F^I</math>; thus, stable contacts with small values of this energy difference (large values of <math>E_F^I</math>) could be important in designing nonalloyed ohmic contacts.</p> <p>Very thin (<math>\sim 10\text{\AA}</math>) epitaxial layers of <math>\text{Ge}</math> that incorporate <math>\text{As}</math> have been found to produce exceptionally large values of <math>E_F^I</math>, 1.0-1.2 eV relative to the valence band maximum (as determined by x-ray photoelectron spectroscopy). Thick model contacts that include layered structures of Au, Ge, and Ni in various combinations have been used to establish conditions under which these large <math>E_F^I</math> values can be preserved (as determined by current-voltage measurements). The results question the usual assumption of a near mid-gap <math>E_F^I</math> position for the widely used alloyed AuGeNi ohmic contact and offer an alternative explanation for the mechanism of ohmic contact formation.</p>			
20. DISTRIBUTION/AVAILABILITY OF ABSTRACT UNCLASSIFIED/UNLIMITED <input type="checkbox"/> SAME AS RPT. <input checked="" type="checkbox"/> DTIC USERS <input type="checkbox"/>		21. ABSTRACT SECURITY CLASSIFICATION <b>UNCLASSIFIED</b>	
22a. NAME OF RESPONSIBLE INDIVIDUAL <b>Capt Mollay</b>		22b. TELEPHONE NUMBER (Include Area Code) <b>(202) 767-4231</b>	22c. OFFICE SYMBOL <b>NE</b>

DD FORM 1473, 83 APR

EDITION OF 1 JAN 73 IS OBSOLETE

UNCLASSIFIED

SECURITY CLASSIFICATION OF THIS PAGE



## TABLE OF CONTENTS

	<u>Page</u>
1.0 INTRODUCTION .....	1
2.0 EXPERIMENTAL PROCEDURE .....	3
3.0 RESULTS .....	7
3.1 Fermi Level Modification by Thin Ge Layers .....	7
3.2 Observed Fermi Levels for Thin Composite Layers .....	9
3.3 Barrier Height Modification for Thick Contacts .....	10
3.4 Clean (100) Surfaces .....	13
4.0 SUMMARY AND CONCLUSIONS .....	15
5.0 REFERENCES .....	16
6.0 APPENDIX .....	18



Accession For	
NTIS CRA&I	<input checked="checked" type="checkbox"/>
DTIC TAB	<input type="checkbox"/>
Unannounced	<input type="checkbox"/>
Justification	
By	
Distribution/	
Availability Codes	
Dist	Avail and/or Special
A-1	



## LIST OF FIGURES

<u>Figure</u>		<u>Page</u>
1	Analysis method of Ga3d peak used to determine $E_F^1$ from XPS data. ....	5
2	Schematic band diagram that illustrates the use of XPS to determine $E_F^1$ . ....	5
3	XPS Ga3d core level spectra for various thin overlayer structures on thermally cleaned n-GaAs(100) surfaces. ....	10
4	Representative I-V data for a selection of contacts to GaAs. ....	11



## LIST OF TABLES

<u>Table</u>		<u>Page</u>
1	Values of $E_{\text{GaAs}}$ , $E_{\text{Ga3d}}^1$ and Preparation Conditions .....	8
2	Interface Structure, $E_F^1$ Following Ge Deposition, Barrier Height and Ideality Factor for Several Thick Contacts .....	12
3	Linewidths and Core Level Splittings Observed on Thermally Cleaned GaAs(100) Surfaces .....	14



## 1.0 INTRODUCTION

This is the annual report for Contract No. F49620-85-C-0120, "Ohmic Contacts to  $\text{Ga}_{1-x}\text{Al}_x\text{As}$  for High Temperature Applications," that covers the time period July 1, 1985 through June 30, 1986. The most widely used ohmic contact to n-GaAs is the alloyed AuGeNi metallization.<sup>1</sup> Several studies have shown that these alloyed contacts have multiphase structures with the phase size and composition being dependent on alloying conditions.<sup>2,3</sup> The alloying process involves melting and resolidification of material on a  $10^3\text{\AA}$  dimensional scale; the process requires careful control to achieve repeatability for the heterogeneous contacts.

New types of GaAs heterostructure devices are being developed to accommodate very high frequency applications; these new devices include the heterojunction bipolar transistor (HBT). Current gain cutoff frequencies of 55 GHz have been reported for  $\text{Ga}_{1-x}\text{Al}_x\text{As}$  HBTs and frequency dividers (1/4) have been operated up to 16 GHz.<sup>4</sup> To increase frequency and circuit complexity, device dimensions must decrease, which places increasing importance on ohmic contact quality and uniformity. In addition, self-aligned processing techniques based on ion implantation will require contacts to have excellent thermal stability in order to withstand the annealing conditions necessary to activate the ion-implanted dopants. There is a need to develop nonalloyed ohmic contacts to  $\text{Ga}_{1-x}\text{Al}_x\text{As}$  that have good high temperature stability.

The mechanism by which the commonly used AuGeNi metallization forms ohmic contacts is not well known. It is generally observed that metal contacts to n-GaAs have a narrow range of Schottky barrier heights ( $\phi_B$ ) of about 0.7 to 0.9 eV. Therefore, it is usually assumed that a sizeable Schottky barrier exists at the metal/GaAs interface and that a tunneling contact is formed by heavy Ge doping of the GaAs near-interface region.<sup>5,6</sup> The tunneling contact model<sup>7</sup> has  $\rho_c \sim \exp(C \phi_B N_D^{-1/2})$ , where  $\rho_c$  is the specific contact resistance,  $N_D$  is the net donor concentration, and C is a constant. Thus, for a fixed  $\phi_B$ ,  $\rho_c$  is minimized by maximizing  $N_D$ . For n-type GaAs with a near maximum possible donor concentration of  $\sim 5 \times 10^{19} \text{ cm}^{-3}$  and  $\phi_B \sim 0.7 \text{ eV}$ , one can estimate a lower limit of  $\sim 1.5 \times 10^{-6} \Omega\text{-cm}^2$  for  $\rho_c$ .<sup>8</sup> This lower limit is not acceptable for some GaAs heterostructure device applications.





Because  $\rho_c$  for a tunneling contact depends exponentially on  $\phi_B$ , the development of a stable low barrier GaAs interface could be important in the design of non-alloyed ohmic contacts. Although the interface Fermi level ( $E_F^i$ ) for GaAs (measured relative to the valence band maximum,  $E_v$ ) is generally confined to a fairly narrow range, there is evidence that at some interfaces, a much larger  $E_F^i$  range can be obtained.<sup>9-14</sup> For certain, thin ( $\sim 10-40\text{\AA}$ ) Ge overlayers on clean GaAs surfaces,  $E_F^i$  can be  $> 1.0\text{ eV}$ .<sup>11,12</sup> If this large value of  $E_F^i$  (which corresponds to a low  $\phi_B$ ) can be obtained in a tunnel contact, it could significantly lower  $\rho_c$  for a given  $N_D$ . Thus, an initial objective of the program was to investigate conditions needed to obtain interfaces with large  $E_F^i$  and to explore means of retaining this interface characteristic in thick contacts.



## 2.0 EXPERIMENTAL PROCEDURE

The interfaces studied in this program were prepared under ultrahigh vacuum conditions (base pressure  $10^{-10}$  Torr) in a custom sample preparation chamber attached to an HP 5950A x-ray photoelectron spectroscopy (XPS) system. A monochromatic Al K $\alpha$  ( $h\nu = 1486.6$  eV) x-ray source was used and the effective photoelectron escape depth was  $\sim 16\text{\AA}$ . During interface formation, XPS spectra of the Ga3d, As3d and Ge3d core-level peaks were obtained. At the conclusion of an interface characterization, a thick ( $\geq 10^3\text{\AA}$ ) Au metal layer was evaporated onto the sample surface and an absolute  $E_F^\dagger$  value was obtained by indexing the Au 4f $_{7/2}$  XPS peak position to 84.00 eV;<sup>15</sup> in a few cases, a thick Ni layer was evaporated onto the sample instead of Au and  $E_F^\dagger$  was obtained by indexing the Ni 2p $_{3/2}$  XPS line to 852.72 eV (a value experimentally determined by depositing thick Au on Ni samples and again indexing Au 4f $_{7/2}$  to 84.00 eV).

The bulk n-type GaAs(100) material used was liquid encapsulated Czochralski grown ( $\sim 5 \times 10^{16} \text{ cm}^{-3}$  Se). Samples were prepared by etching in fresh 4H $_2$ SO $_4$ :1H $_2$ O $_2$ :1H $_2$ O solution for  $\sim 30$  s to remove polishing damage, mounted on a Mo plate with In and immediately inserted into the XPS system. The  $\sim 10\text{\AA}$  native oxide layer was removed by momentary heating either in vacuum or in an As $_4$  overpressure to the minimum necessary temperature ( $\sim 550^\circ\text{C}$ ); this heating step also forms an ohmic contact between the GaAs and the Mo plate. The thermally cleaned surface is ordered (displays a characteristic low energy electron diffraction (LEED) pattern) and shown by XPS to be free of oxygen, carbon or other contaminants. Resistivity heated tungsten wire baskets were used to deposit Ge, Au and Ni onto samples; small quartz ovens were used to provide sources of As $_4$  and Te. Layers of NiAs $_x$  were formed by depositing Ni onto a room-temperature substrate in a  $10^{-7}$ - $10^{-6}$  Torr As $_4$  overpressure; XPS analysis indicated that the resulting Ni and As layer was As-rich and, thus, a compound(s) of the form NiAs $_x$  was present. After XPS analysis of thin overlayers, a total overlayer thickness of  $> 2000\text{\AA}$  was deposited. To facilitate current-voltage (I-V) measurement of  $\phi_B$ , circular  $2.54 \times 10^{-2}$  cm diameter contacts were defined by using photolithography and chemical etching.



The Ga3d XPS core level peak data were utilized to determine  $E_F^1$  for GaAs samples with thin overlayers. A background function proportional to the integrated photoelectron intensity was first subtracted from the XPS spectrum in the vicinity of the Ga3d peak. The resulting peak was least-squares fit to a third order polynomial near the peak maximum and near the half-height on both sides of the peak to determine the peak center (position of the half width point at half height) and the peak width,  $r$  (the full width at half height). A representative example of this analysis is shown in Fig. 1. A schematic band diagram that illustrates the use of XPS to measure  $E_F^1$  is shown in Fig. 2. For moderately doped GaAs, the depletion width  $W$  is  $\sim 10^3 \text{ \AA}$  which is much larger than the effective photoelectron escape depth so that the effect of band bending on the measured position of the Ga3d peak in GaAs ( $E_{\text{Ga3d}}^{\text{GaAs}}$ ) can be ignored. In Fig. 2, the GaAs conduction band minimum is  $E_C^{\text{GaAs}}$  and it should be noted that the binding energy ( $E_B$ ) scale is referenced to the sample  $E_F$ . The Ga3d core level to  $E_V^{\text{GaAs}}$  binding energy difference has been determined to be  $18.75 \pm 0.03 \text{ eV}^{16,17}$  so that  $E_F^1$  is determined from

$$E_F^1 = E_{\text{Ga3d}}^{\text{GaAs}} - 18.75 \text{ eV.} \quad (1)$$

Further details on the use of XPS to measure  $E_F^1$  can be found elsewhere.<sup>9</sup>

I-V data were obtained in 0.01 V forward bias increments by using an automatic system that includes a HP4140B pA meter/voltage source. Both room temperature and low temperature measurements were performed. The low temperature cold stage uses a nitrogen gas Joule-Thompson expansion system. Low temperature measurements were necessary to analyze the low  $\phi_B$  samples. The I-V data were analyzed by use of the Schottky barrier thermionic emission model with

$$I = I_s \exp(qV/nkT) [1 - \exp(-qV/kT)]A \quad (2)$$

where both the ideality factor  $n$  (at  $T = 295\text{K}$ ,  $n \sim 1.02$  is ideal; however, there is often an increase in  $n$  at low  $T$ ) and  $I_s$  (the saturation current) were determined by a least-squares fit. The  $\phi_B$  was extracted from  $I_s$  by

$$I_s = S A^* T^2 \exp[-q(\phi_B - \Delta\phi)/kT]A \quad (3)$$

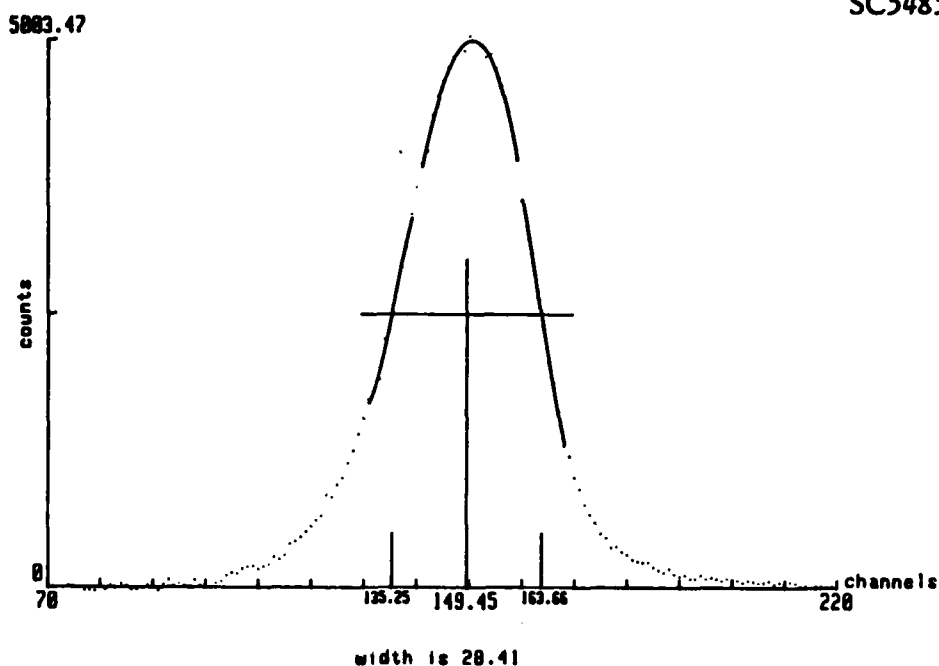


Fig. 1 Analysis method of Ga3d peak used to determine  $E_F^i$  from XPS data. Curves are least-square fits to third order polynomials; the peak center and full width at half maximum are indicated.

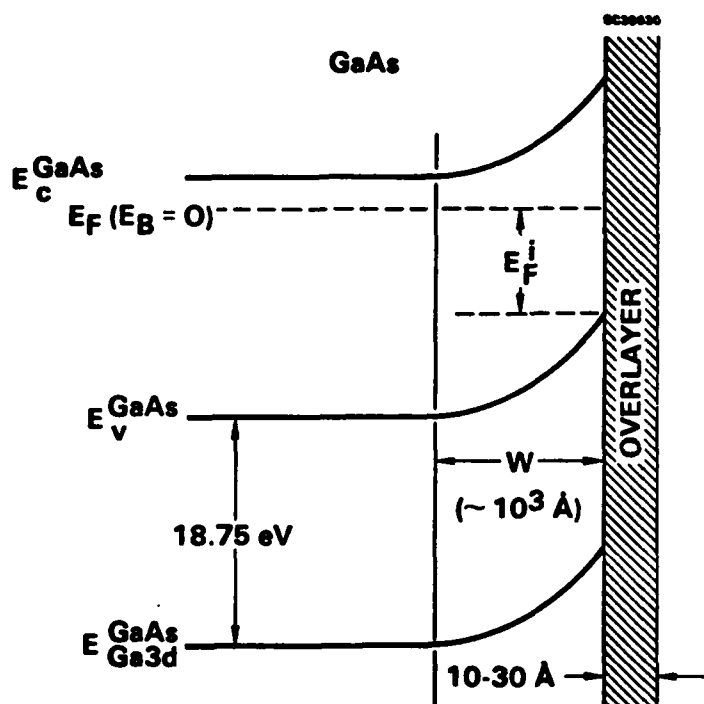


Fig. 2 Schematic band diagram that illustrates the use of XPS to determine  $E_F^i$ .



where  $S$  is the contact area,  $A^* = 8.16$  is the effective Richardson constant, and  $\Delta\phi$  is the calculated image force correction ( $\Delta\phi = \pm 0.04$  eV for  $\phi_B \geq 0.7$  eV and  $+0.03$  eV for  $\phi_B < 0.7$  eV). Good reproducibility of results between contacts on a given sample was observed and thus average values (approximately seven contacts per sample) of  $\phi_B$  and  $n$  were determined; the measurement uncertainty for  $\phi_B$  was  $< \pm 0.01$  eV.



### 3.0 RESULTS

In this section, XPS measurements of  $E_F^1$  for thin layers of Ge on n-GaAs(100) are described that demonstrate a large range of values. It is shown that large  $E_F^1$  values can be preserved for some thin composite layers. I-V measurements on thick contacts are found to correlate well with the XPS results and establish that low values of  $\phi_B$  can be retained in some cases. Finally, XPS measurements on the thermally clean GaAs(100) surface suggest that surface chemical shifts may be quite different than observed on the GaAs(110) surface.

#### 3.1 Fermi Level Modification by Thin Ge Layers

A wide range of  $E_F^1$  values for thin Ge overlayers on clean GaAs surfaces has been reported.<sup>11,12,19,20</sup> It has been concluded that As doping of the Ge overlayer caused by details of the preparation conditions is important in determining  $E_F^1$  while deposition-induced defects are not.<sup>21</sup> This phenomenon was investigated for several Ge overlayers deposited onto thermally cleaned GaAs(100) substrates. The substrates were either cleaned in vacuum or in an  $As_4$  background pressure. The Ge layers were deposited either in vacuum or in the presence of  $As_4$ ; these latter layers are designated Ge(As). The GaAs substrate temperature was constant during a Ge deposition, but ranged between room temperature and 325°C for different samples. The deposited Ge and Ge(As) overlayer thicknesses were estimated from the substrate Ga3d photoelectron intensity attenuation. A LEED pattern from the Ge and Ge(As) layers was observed for substrate deposition temperatures between 200 and 325°C, although a high background was present at 200°C. The room temperature deposited Ge(As) did not exhibit a LEED pattern and XPS analysis indicated a large excess of As in the deposited layer.

The Ge and Ge(As) overlayer preparation conditions and the observed values of  $E_{Ga3d}^{GaAs}$  are given in Table 1; also given are the values of  $E_F^1$  evaluated from Eq. (1). For comparison, the average values of  $E_{Ga3d}^{GaAs}$  and  $E_F^1$  observed on the thermally cleaned GaAs(100) surfaces before overlayer deposition are also given in the table. The Ge(As) layers deposited between 200 and 325°C, where As incorporation presumably makes the Ge n-type, exhibited a  $E_F^1$  range of 1.03-1.21 eV. In contrast, the  $E_F^1$  range for Ge(As)



Table I  
Values of  $E_{\text{GaAs}}^{\text{Ga3d}}$ ,  $E_F^i$  and Preparation Conditions

Sample No.	Overlayer	Deposition Temp. (°C)	Overlayer Thickness (Å)	Background Pressure During Deposition (Torr)	$E_{\text{GaAs}}^{\text{Ga3d}}$ (eV)	$E_F^i$ (eV)
	Thermally Clean (ave. value)	---	---	---	19.46	0.71
1	Ge	200	9	Vacuum	19.45	0.70
2	Ge <sup>a</sup>	200	10	Vacuum	19.87	1.12
3	Ge	325	9	Vacuum	19.20	0.45
	Sample No. 3 + Exposure to 30 L As <sub>4</sub> at 325°C	---	---	---	19.26	0.51
4	Ge(As)	R.T.	26	10 <sup>-7</sup> As <sub>4</sub>	19.49	0.74
5	Ge(As)	200	10	10 <sup>-7</sup> As <sub>4</sub>	19.82	1.07
6	Ge(As)	200	7	10 <sup>-7</sup> As <sub>4</sub>	19.79	1.04
7	Ge(As) <sup>b</sup>	200	9	10 <sup>-7</sup> As <sub>4</sub>	19.78	1.03
8	Ge(As)	200	11	10 <sup>-7</sup> As <sub>4</sub>	19.78	1.03
9	Ge(As) <sup>a</sup>	200	4	10 <sup>-7</sup> As <sub>4</sub>	19.78	1.03
10	Ge(As)	250	9	10 <sup>-7</sup> As <sub>4</sub>	19.96	1.21
11	Ge(As)	250	9	10 <sup>-7</sup> As <sub>4</sub>	19.90	1.15
12	Ge(As)	250	8	10 <sup>-7</sup> As <sub>4</sub>	19.78	1.03
13	Ge(As)	250	7	10 <sup>-7</sup> As <sub>4</sub>	19.89	1.14
14	Ge(As)	325	11	10 <sup>-7</sup> As <sub>4</sub>	19.85	1.10

a. Substrate cleaned in 10<sup>-6</sup> Torr As<sub>4</sub>

b. Substrate cleaned in 10<sup>-7</sup> Torr As<sub>4</sub>



deposited at room temperature and for Ge deposited between 200 and 325°C was 0.45–0.75 eV. It is interesting to note that Ge deposited at 200°C in vacuum (Sample No. 2) onto a GaAs substrate thermally cleaned in the presence of  $10^{-6}$  Torr  $As_4$  exhibited  $E_F^1 = 1.12$ , presumably due to increased As incorporation into the subsequently grown Ge layer and/or decreased Ga incorporation. Also, exposure of Sample No. 3 to 30L of  $As_4$  following Ge deposition had only a small effect on the observed  $E_F^1$  value.

### 3.2 Observed Fermi Levels for Thin Composite Layers

In Section 3.1, it was noted that very large values (1.03–1.21 eV) of  $E_F^1$  could be obtained for Ge(As) layers formed on thermally cleaned n-GaAs(100) between 200 and 325°C. If these  $E_F^1$  values could be retained in thick contacts, the corresponding interfaces could have n-type ohmic contact applications.

The effect of depositing thin layers of  $NiAs_x$ , Te, Au and Ni onto Ge(As)/GaAs samples was investigated. The  $NiAs_x$ , Au and Ni layers were chosen as they are constituents of the AuGeNi ohmic contact metallization; Te was investigated because a previous study<sup>13</sup> of large  $E_F^1$  n-GaAs(100) interfaces formed by metal-chalcogen overlayers had demonstrated that a Te layer could preserve a low band bending interface characteristic.

The Ga3d XPS spectra that provide results for the composite layer experiments are shown in Fig. 3. The first three spectra are from the same sample (Sample No. 11 of Table 1) after sequential layer depositions. For reference, the top spectrum is from the thermally cleaned surface and the vertical line marks the center of the clean surface Ga3d peak at 19.47 eV ( $E_F^1 = 0.72$  eV). After depositing 9Å of Ge(As) at 250°C,  $E_{Ga3d}^{GaAs}$  shifts by 0.43 eV to higher  $E_B$ , which corresponds to an increase in  $E_F^1$  to 1.15 eV. Subsequent deposition of 9Å of  $NiAs_x$  onto this sample produced essentially no change in  $E_{Ga3d}^{GaAs}$ , and thus, no change in  $E_F^1$ . A similar result was obtained when Te was deposited onto a Ge(As)/GaAs sample (see fourth spectrum from top in Fig. 3). As with the  $NiAs_x$  layer, the low band bending GaAs interface is preserved. The situation is dramatically different when either Au or Ni is deposited onto a low band bending Ge(As)/GaAs sample (see two bottom spectra of Fig. 3). In each case,  $E_F^1$  decreased by ~0.4 eV, which indicates that the low band bending condition was removed (the low  $E_B$  shoulder on the





last peak in Fig. 3 suggests that Ni has reached the GaAs interface to produce a chemical reaction). Thus, it is concluded that at least some thin composite layers are capable of preserving the desirable low band bending characteristic.

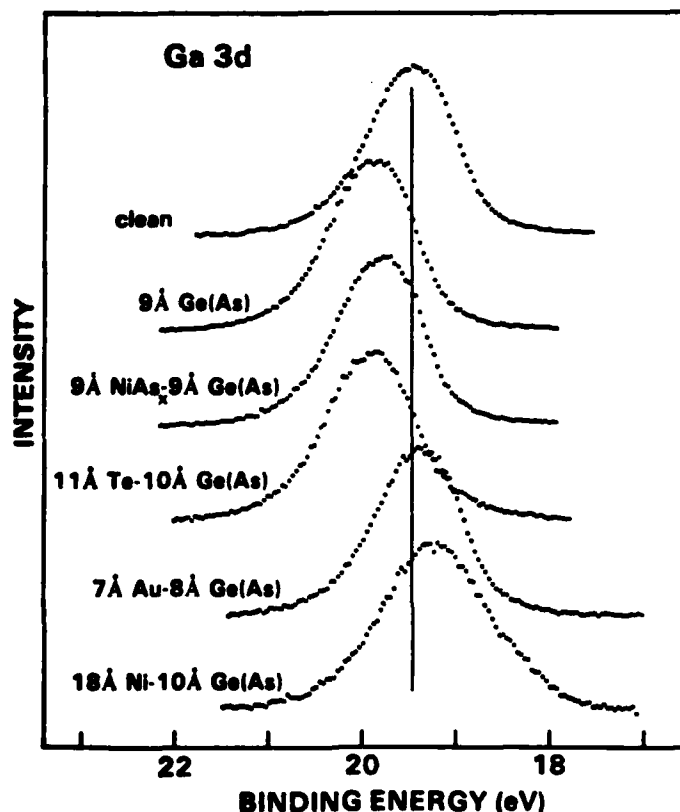


Fig. 3 XPS Ga3d core level spectra for various thin overlayer structures on thermally cleaned n-GaAs(100) surfaces. Upper three spectra are for successive depositions on the same sample.

### 3.3 Barrier Height Modification for Thick Contacts

If large values of  $E_F^1$  can be preserved at some n-GaAs(100) interfaces, it should be possible to observe low values of  $\phi_B$  by I-V. The relation  $\phi_B = E_g - E_F^1$ , where the GaAs band gap  $E_g = 1.43$  eV, indicates that  $\phi_B$  in the 0.2-0.4 eV range should be obtained. Several thick contact structures were formed to investigate this question. Representative I-V data are shown in Fig. 4. The samples labeled as Au-ideal, Ni-ideal, and NiAs<sub>x</sub>-ideal were prepared by depositing Au, Ni or NiAs<sub>x</sub> directly onto thermally



cleaned GaAs. As noted in Table 2, these samples all exhibit large values of  $\phi_B$  in the 0.8-0.9 eV range that is common for GaAs.

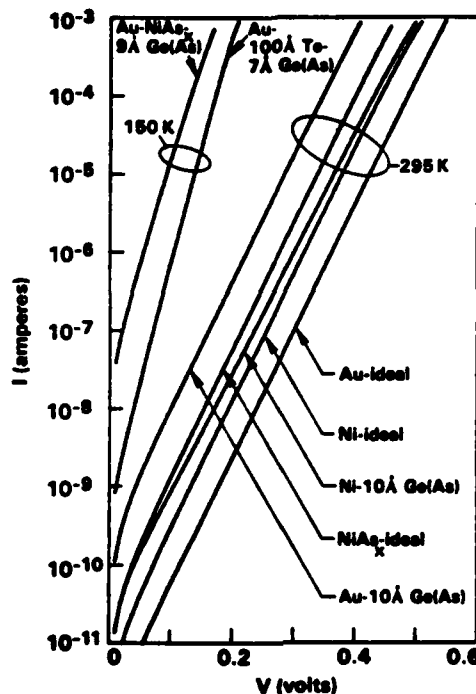


Fig. 4 Representative I-V data for a selection of contacts to GaAs. Contact composition is noted in the figure and area was  $5.07 \times 10^{-4} \text{ cm}^2$ .

Data for four other samples are shown in Fig. 4. For these samples, an initially large  $E_F^1$  was obtained by depositing a thin Ge(As) layer onto the thermally cleaned GaAs(100) surface. Following the Ge(As) deposition, XPS was used to measure  $E_F^1$ , as noted in Table 2. When either Au or Ni was deposited directly onto the Ge(As)/GaAs(100) samples, the low band bending (large  $E_F^1$ ) condition was destroyed and values of  $\phi_B$  in the 0.6 to 0.8 eV range were observed (see Table 2). However, if an intervening layer of NiAs<sub>x</sub> or Te was deposited before the Au deposition, very low values of  $\phi_B$  in the 0.2-0.4 eV range could be obtained. As shown in Fig. 4 and indicated in Table 2, it was necessary to lower the sample temperature to measure these low values of  $\phi_B$ . Thus, in agreement with the XPS results of Section 3.2, it is possible to preserve the high  $E_F^1$  condition associated with Ge(As)/GaAs samples by introducing intervening NiAs<sub>x</sub> or Te layers to prevent Au or Ni from reaching the GaAs interface. These intervening



layers apparently act as diffusion barriers while also providing a conducting electrical contact.

**Table 2**  
**Interface Structure,  $E_F^{\dagger}$  Following Ge Deposition, Barrier Height and**  
**Ideality Factor for Several Thick Contacts**

Interface Structure	Ge Deposition Temperature (°C)	$E_F^{\dagger a}$ (eV)	$\phi_B^{b,c}$ (eV)	n
Au - NiAs <sub>x</sub> - 9Å Ge(As)	200	1.03	0.31 <sup>d</sup>	1.27
Au - NiAs <sub>x</sub> - 11Å Ge(As)	200	1.03	0.35 <sup>d</sup>	1.23
Au - NiAs <sub>x</sub> - 9Å Ge(As)	250	1.15	0.39 <sup>d</sup>	1.11
Au - 100Å Te - 10Å Ge(As)	200	1.12	0.23 <sup>e</sup>	1.33
Au - 100Å Te - 9Å Ge(As)	250	1.21	0.39 <sup>d</sup>	1.08
Au - 100Å Te - 7Å Ge(As)	325	1.10	0.36 <sup>d</sup>	1.10
Au - 10Å Ge(As)	200	1.07	0.76	1.05
Au - 8Å Ge(As)	250	1.03	0.61	1.05
Au - 9Å Ge(As)	325	1.21	0.64	1.05
Ni - 10Å Ge(As)	200	1.04	0.81	1.11
Au - 100Å Te - 9Å Ge	200	0.70	0.65	1.06
Au - 9Å Ge	325	0.45	0.71	1.12
NiAs <sub>x</sub> -ideal	---	---	0.80	1.04
Ni-ideal	---	---	0.84	1.05
Au-ideal	---	---	0.89	1.05

a. Measured by XPS following Ge or Ge(As) deposition

b. Includes image force correction

c. Measured at 295K, unless noted

d. T = 150K

e. T = 100K



### 3.4 Clean (100) Surfaces

XPS was used to characterize the thermally cleaned GaAs(100) surfaces prior to overlayer deposition. The observed Ga3d and As3d linewidths and core level splittings are given in Table 3. On the clean GaAs(110) surface, the observed core level splitting is  $(E_{\text{As3d}}^{\text{GaAs}} - E_{\text{Ga3d}}^{\text{GaAs}})_{110} = 21.92 \text{ eV}.$ <sup>16</sup> When this observed splitting is corrected for the known surface chemical shifts of Ga3d and As3d on the GaAs(110) surface,<sup>22</sup> the derived bulk GaAs core level splitting is  $(E_{\text{As3d}}^{\text{GaAs}} - E_{\text{Ga3d}}^{\text{GaAs}})_{\text{bulk}} = 21.99 \text{ eV}.$ <sup>16</sup> In contrast to the GaAs(110) surface, the average core level splitting for the GaAs(100) surface is larger than the bulk value,  $(E_{\text{As3d}}^{\text{GaAs}} - E_{\text{Ga3d}}^{\text{GaAs}})_{100} = 22.05 \text{ eV}.$  Although surface chemical shift studies have not been reported for the GaAs(100) surface, this result suggests that these shifts may be quite different than those observed on the (110) surface. Surface chemical shifts would have to be considered in determining  $E_F^1$  for the thermally clean GaAs(100) surface. If it is arbitrarily assumed that surface chemical shifts increase  $E_{\text{Ga3d}}^{\text{GaAs}}$  by +0.03 eV, and decrease  $E_{\text{As3d}}^{\text{GaAs}}$  by -0.03 eV relative to the bulk values, the average value of  $E_F^1$  quoted in Table 1 for the thermally cleaned GaAs(100) surface would have to be increased by 0.03 eV.



Table 3  
Linewidths and Core Level Splittings Observed  
on Thermally Cleaned GaAs(100) Surfaces

Sample No.	As <sub>4</sub> Pressure During Cleaning (Torr)	$\Gamma_{\text{Ga}3d}$ (eV)	$\Gamma_{\text{As}3d}$ (eV)	$E_{\text{GaAs As}3d} - E_{\text{GaAs Ga}3d}$ (eV)
1	UHV	1.14	1.42	22.05
2	10 <sup>-6</sup>	1.10	1.48	22.07
3	UHV	1.09	1.37	22.07
4	UHV	1.15	1.45	22.07
5	UHV	1.14	1.42	22.02
6	UHV	1.11	1.46	22.06
7	10 <sup>-7</sup>	1.19	1.48	22.07
8	UHV	1.12	1.41	22.06
9	10 <sup>-6</sup>	1.11	1.44	22.06
10	UHV	1.13	1.45	21.97
11	UHV	1.09	1.42	22.05
12	UHV	1.16	1.42	22.02
13	UHV	1.11	1.45	22.10
14	UHV	1.18	1.45	22.04
Ave. Values	---	1.13	1.44	22.05



#### 4.0 SUMMARY AND CONCLUSIONS

Thin layers of Ge that incorporate As have been found to produce exceptionally low  $\phi_B$  interfaces on n-GaAs(100). Under suitable conditions, the low  $\phi_B$  interface can be retained in thick contacts as demonstrated by I-V measurements. The role of Ge and As in producing the low  $\phi_B$  contacts as well as the thermal stability of the contacts needs to be explored. The low  $\phi_B$  interfaces offer interesting possibilities for the design of nonalloyed tunnel ohmic contacts.

The mechanism of ohmic contact formation to n-GaAs for the widely used AuGeNi metallization is not well understood. In a careful electron microscopy investigation,<sup>2</sup>  $\rho_C$  was found to depend on the relative contact area of several phases. It was concluded that a low  $\rho_C$  was achieved when the  $Ni_2GeAs$  phase dominates because of enhanced Ge doping of the near GaAs interface region. The observation that thin ( $\sim 10\text{\AA}$ ) Ge(As) layers can markedly reduce  $\phi_B$  suggests an alternate explanation. The  $Ni_2GeAs$  and  $NiAs_x$  phases may be separated from the GaAs by a very thin unobserved interface layer of Ge(As) and are thus associated with a low  $\phi_B$  region. With this model, a low  $\rho_C$  for the alloyed AuGeNi ohmic contact is obtained when the interface area of phases associated with a low  $\phi_B$  is greatest.



## 5.0 REFERENCES

1. N. Braslau, J.B. Gunn and J.L. Staples, Solid State Electron. 10, 381 (1967).
2. T.S. Kuan, P.E. Batson, T.N. Jackson, H. Rupprecht and E.L. Wilkie, J. Appl. Phys. 54, 6952 (1983).
3. C.J. Palmstrom and D.V. Morgan, Gallium Arsenide, M.J. Howes and D.V. Morgan, eds., Wiley, Chichester, Chapt. 6 (1985), and references therein.
4. M.F. Chang, P.M. Asbeck, K.C. Wang, G.J. Sullivan, N.H. Sheng, J.A. Higgins and D.L. Miller, submitted to Electron Device Letters.
5. N. Braslau, J. Vac. Sci. Tech. 19, 803 (1981).
6. N. Braslau, J. Vac. Sci. Tech. A4, 3085 (1986).
7. C.Y. Chang, Y.K. Fang and S.M. Sze, Solid-State Electron. 14, 541 (1971).
8. See, e.g., C.E.C. Wood, J. Vac. Sci. Tech. 18, 772 (1981).
9. R.W. Grant, J.R. Waldrop, S.P. Kowalczyk and E.A. Kraut, J. Vac. Sci. Tech. 19, 477 (1981).
10. J. Massies, J. Chaplart, M. Laviro and N.T. Linh, Appl. Phys. Lett. 38, 693 (1981).
11. H. Brugger, F. Schäffler and G. Abstreiter, Phys. Rev. Lett. 52, 141 (1984).
12. P. Chiaradia, A.D. Katnani, H.W. Sang, Jr. and R.S. Bauer, Phys. Rev. Lett. 52, 1246 (1984).
13. J.R. Waldrop, Appl. Phys. Lett. 47, 1301 (1985).



14. S.D. Offsey, J.M. Woodall, A.C. Warren, P.D. Kirchner, T.I. Chappel and G.D. Pettit, Appl. Phys. Lett. 48, 475 (1986).
15. F.R. McFeely, S.P. Kowalczyk, L. Ley, R.A. Pollak and D.A. Shirley, Phys. Rev. B7, 5228 (1973).
16. E.A. Kraut, R.W. Grant, J.R. Waldrop and S.P. Kowalczyk, Phys. Rev. B28, 1965 (1983).
17. J.R. Waldrop, R.W. Grant and E.A. Kraut, J. Vac. Sci. Tech. (in press); the original value of  $E_{\text{GaAs}}^{\text{Ga3d}} - E_v^{\text{GaAs}}$  quoted in Ref. 16 has been revised by -0.05 eV.
18. E.H. Rhoderick, Metal-Semiconductor Contacts, Clarendon, Oxford (1977).
19. W. Mönch and H. Gant, Phys. Rev. Lett. 48, 512 (1982).
20. S.P. Kowalczyk, R.W. Grant, J.R. Waldrop and E.A. Kraut, J. Vac. Sci. Tech. B1, 684 (1983).
21. A.D. Katnani, P. Chiaradia, H.W. Sang, Jr., and R.S. Bauer, J. Electron. Mat. 14, 25 (1985).
22. D.E. Eastman, T.-C. Chiang, P. Heimann and F.J. Himpsel, Phys. Rev. Lett. 45, 656 (1980).





**Rockwell International**  
**Science Center**  
**SC5485.AR**

## **6.0 APPENDIX**

This appendix contains a reprint that discusses work supported by this contract during the reporting period. The reprint is entitled, "Correlation of Interface Composition and Barrier Height for Model AuGeNi Contacts to GaAs," J.R. Waldrop and R.W. Grant, Appl. Phys. Lett. 50, 250 (1987).

# Correlation of interface composition and barrier height for model AuGeNi contacts to GaAs

J. R. Waldrop and R. W. Grant

Rockwell International Corporation, Thousand Oaks, California 91360

(Received 23 July 1986; accepted for publication 2 December 1986)

Model contacts to GaAs that include nonalloyed layered structures of Au, Ge, and Ni in various combinations are used to establish a correlation between interface composition and large changes in barrier height  $\phi_B$ . The interface Fermi level  $E_F$  and chemistry during initial contact formation were investigated by x-ray photoemission spectroscopy; the corresponding  $\phi_B$  for the thick contact was obtained by current-voltage ( $I$ - $V$ ) measurement. The circumstances under which a thin ( $\sim 10$  Å) Ge layer at the GaAs interface can produce  $\phi_B = \sim 0.25$ – $0.4$  eV (as measured by  $I$ - $V$ ) are described. For all model contacts examined a  $\phi_B$  range from  $\sim 0.25$  to  $0.9$  eV is observed. This result questions the usual assumption of a relatively fixed  $\phi_B$  of  $\sim 0.8$  eV for the alloyed AuGeNi contact and offers an alternative explanation for the mechanism of ohmic contact formation. The conditions that define the exceptionally low  $\phi_B$  contacts provide a guide for the design of nonalloyed tunnel ohmic contacts.

The alloyed AuGeNi metallization<sup>1</sup> is widely used as an ohmic contact to  $n$ -type GaAs. The complex contact structure consists of several phases whose individual size and composition depend on the alloying time and temperature.<sup>2–5</sup> The familiar ohmic contact tunneling<sup>6</sup> model that gives<sup>7</sup>  $\rho_c \propto \exp(a\phi_B/N_D^{1/2})$ , where  $\rho_c$  is the specific contact resistance,  $\phi_B$  is the interface barrier height,  $N_D$  is the donor concentration in the GaAs ( $> 5 \times 10^{18}$  cm<sup>-3</sup>), and  $a = 5 \times 10^{10}$  cm<sup>-3/2</sup> eV<sup>-1</sup>, is troublesome to apply quantitatively to the alloyed contact. This difficulty arises from not knowing precisely either  $\phi_B$  or the effect of Ge, Au, or Ni indiffusion on  $N_D$ . It is usually assumed that  $\phi_B$  is inevitably  $\sim 0.7$ – $0.9$  eV because the Schottky barrier height<sup>8,9</sup> for most metal contacts to GaAs is in this range. According to this viewpoint  $\rho_c$  is reduced by maximizing  $N_D$ . However, for certain thin ( $\sim 10$ – $40$  Å) Ge overlayers on clean GaAs surfaces the interface Fermi energy  $E_F$  can be  $> 1$  eV.<sup>10,11</sup> Hence, if such a high  $E_F$  state (low  $\phi_B$ ) can be attained in a tunnel AuGeNi ohmic contact then  $\rho_c$  would be substantially reduced for a given  $N_D$ .

This letter reports an investigation of model AuGeNi contacts to GaAs that involve layered structures designed to correlate interface composition with  $\phi_B$ . The contacts were not alloyed to retain interfaces of controlled composition. The interface chemistry and  $E_F$  during initial contact formation were observed by x-ray photoemission spectroscopy (XPS); the corresponding  $\phi_B$  for a thick contact was obtained by current-voltage ( $I$ - $V$ ) measurement. Since the current transport for a tunnel contact depends on both  $\phi_B$  and  $N_D$ , GaAs with  $N_D$  appropriate for thermionic emission transport ( $< 10^{17}$  cm<sup>-3</sup>) was used to simplify the  $I$ - $V$  analysis.

The contact interfaces were prepared under ultrahigh vacuum conditions ( $10^{-10}$  Torr range base pressure) in an XPS system comprised of a HP5950A electron spectrometer ( $h\nu = 1486.6$  eV monochromatic x-ray source,  $\sim 16$  Å effective photoelectron escape depth) and attached custom sample preparation chamber. During initial contact formation XPS spectra of the Ga 3d and As 3d core level peaks in

the GaAs and of other core level peak spectra appropriate for a given interface composition were obtained.  $I$ - $V$  data were obtained in 0.01 V forward bias increments.

The GaAs (100) material is liquid encapsulated Czochralski grown  $n$  type ( $\sim 5 \times 10^{16}$  cm<sup>-3</sup> Se). To prepare a sample, the GaAs is etched in fresh 4:1:1 H<sub>2</sub>SO<sub>4</sub>:H<sub>2</sub>O<sub>2</sub>:H<sub>2</sub>O solution for  $\sim 30$  s to remove polishing damage, mounted on a Mo plate with In and immediately put into the XPS system. The  $\sim 10$  Å native oxide layer is removed by momentary heating, either in vacuum or in an As overpressure, to the minimum necessary temperature ( $\sim 550$  °C, which also forms an ohmic contact between the GaAs and the Mo plate). This thermally cleaned surface is ordered [displays a characteristic low-energy electron diffraction (LEED) pattern] and is shown by XPS to be free of oxygen, carbon, or other contaminants. The Ge, Au, and Ni were evaporated from W baskets; the As and Te sources were small quartz ovens. The NiAs layers were formed by depositing the Ni onto a room-temperature substrate in a  $10^{-7}$ – $10^{-6}$  Torr As overpressure [although XPS analysis indicates the resulting Ni and As layer is As rich, and thus a compound(s) of the form NiAs<sub>x</sub>, for simplicity it will be referred to as NiAs]. After XPS analysis of thin overlayers, a total overlayer thickness of  $> 2000$  Å was deposited. Circular  $2.54 \times 10^{-2}$  cm diameter contacts were defined by using photolithography and chemical etching.

The representative Ga 3d core level peak data plotted in Fig. 1 show how XPS was used to measure  $E_F$  and to monitor composition during interface formation. The upper three spectra are after sequential treatments to the same sample; the lower three are for three other samples with the indicated overlayer structure (peak heights are normalized). The upper inset in Fig. 2 shows the relationship between the interface Ga 3d core level binding energy in GaAs and  $E_F$ :  $E_F = E_{Ga\ 3d} - 18.80$  eV, where  $(E_{Ga\ 3d} - E_v) = 18.80 \pm 0.03$  eV is the energy difference<sup>12</sup> between the Ga 3d core level and the valence-band maximum. Note that the binding energy  $E_B$  scale is referenced to the sample Fermi energy  $E_F$  (other details on the use of XPS to measure  $E_F$  can be found

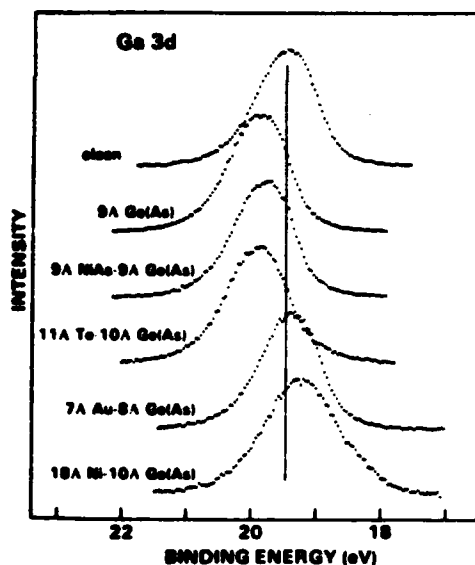


FIG. 1. XPS Ga 3d core level spectra for various thin overlayer structures on initially clean GaAs (100) surfaces. Upper three spectra are for successive depositions on the same sample.

elsewhere).<sup>13</sup> Thus, the vertical line in Fig. 1 that marks the center of the clean surface Ga 3d peak at 19.47 eV is for  $E_F^i(\text{clean}) = 0.67$  eV (the average for 16 samples is 0.66 eV, as indicated in Fig. 2).

After deposition of 9 Å of Ge onto the clean GaAs surface at 250 °C and in  $1 \times 10^{-7}$  Torr As overpressure the Ga 3d peak shifts 0.43 eV to higher binding energy (compare upper two peaks). This shift represents an increase in  $E_F^i$  to 1.10 eV. The  $E_F^i$  for a thin Ge overlayer on clean GaAs will be defined as  $E_F^i(\text{Ge})$ . Figure 2 gives the value of  $E_F^i(\text{Ge})$  for 13 different samples in which  $\sim 10$  Å of Ge was deposited onto clean GaAs (see lower inset) at several different substrate temperatures and As overpressure conditions. These  $E_F^i(\text{Ge})$  data are also tabulated in Table I.

For Ge deposited in a 200–325 °C temperature range under conditions where As incorporation occurs [designat-

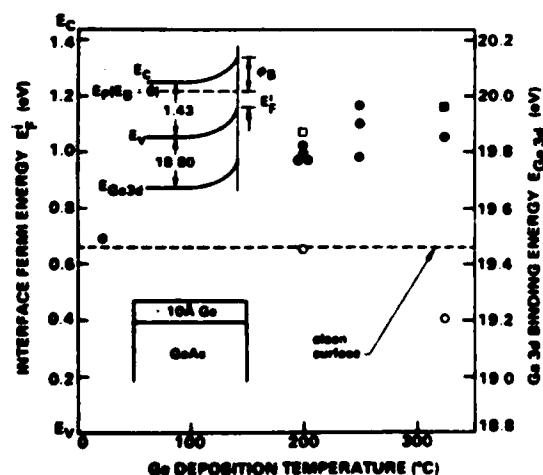


FIG. 2. Interface Fermi energy  $E_F^i(\text{Ge})$  for thin ( $\sim 10$  Å) Ge overlayers deposited on GaAs (100) surfaces at several different temperatures. The closed circles and square are for  $10^{-7}$  and  $10^{-8}$  Torr As overpressure during Ge evaporation, respectively; the open circles are for a GaAs surface cleaned and Ge deposited in vacuum; the open square is for GaAs cleaned in  $10^{-8}$  Torr As and Ge deposited in vacuum.

ed Ge(As)], which presumably makes the Ge  $n$  type.  $E_F^i(\text{Ge}) = 1.0$ – $1.2$  eV. A LEED pattern from the Ge was observed for these layers (with a high background at 200 °C). Room-temperature Ge deposition (no LEED pattern), or 200–325 °C Ge deposition on a vacuum cleaned surface without an As overpressure, yields  $E_F^i(\text{Ge}) = 0.4$ – $0.7$  eV.

The relation  $\phi_B = 1.43$  eV  $- E_F^i$  indicates that barriers in the 0.2–0.4 eV range can be achieved if the low band bending state (high  $E_F^i$ ) can be preserved upon deposition of additional contact material. For example, the third (from top) spectrum in Fig. 1 is for 9 Å of NiAs deposited onto the 9 Å Ge(As) overlayer where  $E_F^i(\text{Ge}) = 1.1$  eV. Essentially no change in the Ga 3d energy, and hence no change in  $E_F^i$ , occurs. To test the generality of this result another conductive nonmetal, Te, was used. When 11 Å of Te is deposited onto a Ge(As) overlayer with high associated  $E_F^i(\text{Ge})$  (fourth spectrum) there is also no change in  $E_F^i$ . The situation is dramatically different when either Au or Ni is deposited directly onto a high  $E_F^i(\text{Ge})$  Ge(As) overlayer (lower two spectra in Fig. 1). In each case  $E_F^i$  shifted from  $E_F^i(\text{Ge}) = \sim 1.1$  eV to  $E_F^i = \sim 0.7$  eV after the metal deposition; thus, the low barrier condition was removed (the low binding energy shoulder in the last peak is due to a Ni-GaAs chemical reaction).

Do the XPS measurements of  $E_F^i$  shifts correlate with the  $I$ - $V$   $\phi_B$  data for the same interfaces? To investigate this question several kinds of model thick contact structures were formed. The types that include Ge are shown on the right side of Fig. 3; in each case an initial Ge overlayer is followed (at room temperature) by the indicated deposi-

TABLE I. Correlation of interface composition and barrier height for model nonalloyed AuGeNi contacts to GaAs.

Interface structure	Ge depos temp (°C)	$E_F^i(\text{Ge})$ (eV)	$\phi_B^{\text{cal}}$ (eV)	$n$
Au-NiAs-9 Å Ge(As)	200	0.98	0.31 <sup>d</sup>	1.27
Au-NiAs-11 Å Ge(As)	200	0.98	0.35 <sup>d</sup>	1.23
Au-NiAs-9 Å Ge(As)	250	1.10	0.39 <sup>d</sup>	1.11
Au-100 Å Te-10 Å Ge(As)	200	1.07	0.23 <sup>e</sup>	1.33
Au-100 Å Te-9 Å Ge(As)	250	1.16	0.39 <sup>d</sup>	1.08
Au-100 Å Te-7 Å Ge(As)	325	1.05	0.36 <sup>d</sup>	1.10
Au-10 Å Ge(As)	200	1.02	0.76	1.05
Au-8 Å Ge(As)	250	0.98	0.61	1.05
Au-9 Å Ge(As)	325	1.16	0.64	1.05
Ni-10 Å Ge(As)	200	0.99	0.81	1.11
Au-100 Å Te-9 Å Ge	200	0.65	0.65	1.06
Au-9 Å Ge	325	0.40	0.71	1.12
Au-100 Å Te <sup>f</sup>	...	...	0.79	1.02
NiAs-ideal	...	...	0.80	1.04
Ni-ideal	...	...	0.84	1.05
Au-ideal	...	...	0.89	1.05

<sup>a</sup> Ge overlayer only.

<sup>b</sup> Includes image force correction, see text.

<sup>c</sup> Measured at  $T = 295$  K unless noted.

<sup>d</sup>  $T = 150$  K.

<sup>e</sup>  $T = 100$  K.

<sup>f</sup> Reference 17.

tions. Not shown are structures without the Ge layer (designated ideal) where Au, Ni, or NiAs is deposited directly onto clean GaAs.

Figure 3 also shows representative  $I$ - $V$  data ( $T = 295$  or  $150$  K, the lower measurement temperature was necessary for low  $\phi_B$ ) that demonstrate the wide range in  $\phi_B$  which is associated with the different contact structures. The  $I$ - $V$  data were analyzed by use of the thermionic emission model<sup>14</sup> for a Schottky barrier:  $I = I_0 \exp(qV/nkT) [1 - \exp(-qV/kT)]^4$ , where both the ideality factor  $n$  ( $n \sim 1.02$  at  $T = 295$  K) is ideal; there is often, however, an increase in  $n$  at low  $T$ <sup>14</sup> and  $I_0$  were determined by a least-squares fit. The barrier height  $\phi_B$  is extracted from  $I_0$  by  $I_0 = SA^*T^2 \exp[-q(\phi_B - \Delta\phi)/kT]$ , where  $S$  is the contact area,  $A^* = 8.16$  is the effective Richardson constant, and  $\Delta\phi$  is the calculated<sup>14</sup> image force correction ( $\Delta\phi = +0.04$  eV for  $\phi_B \geq 0.7$  eV and  $+0.03$  eV for  $\phi_B < 0.7$  eV). Table I lists the average  $\phi_B$  and  $n$  values for the various interface structures ( $\sim$  seven contacts per sample,  $\pm 0.01$  eV measurement uncertainty).

The Au-NiAs-Ge(As) and Au-Te-Ge(As) contacts that have a high  $E'_c$  (Ge) ( $\sim 1.0$ – $1.2$  eV) also have a low  $\phi_B$  ( $\sim 0.25$ – $0.4$  eV). In contrast, the Au-Ge(As) and Ni-Ge(As) contacts that have a similarly high  $E'_c$  (Ge) value have, without an intervening NiAs or Te layer, a high  $\phi_B$  ( $\sim 0.6$ – $0.8$  eV).<sup>15</sup> These values for  $\phi_B$  can be compared to those for the Au and Ni<sup>16</sup> ideal contacts,  $\phi_B$  (Au) =  $0.89$  eV and  $\phi_B$  (Ni) =  $0.84$  eV, and the two contacts where  $E'_c$  (Ge) was  $0.4$  and  $0.65$  eV. Thus, a high  $E'_c$  state induced by a Ge(As) layer can be preserved by a NiAs or Te layer that prevents Au or Ni from reaching the Ge-GaAs interface.

The NiAs-ideal and the Au-100 Å Te<sup>17</sup> contacts have  $\phi_B = 0.79$ – $0.80$  eV, which corresponds to  $E'_c = 0.63$ – $0.64$  eV; this value of  $E'_c$  is essentially that of the clean GaAs surface. Thus, NiAs and Te have no effect on the Ge-GaAs interface electronic structure while also providing a conducting elec-

trical contact (other nonmetal conductors with this property are likely).

In a careful electron microscopy investigation<sup>4</sup> of alloyed AuGeNi contacts  $\rho_c$  was found to depend on the relative contact areas of several Ni<sub>3</sub>GeAs, NiAs, and Au(Ga,As) phases. It was concluded that a low  $\rho_c$  is achieved when the Ni<sub>3</sub>GeAs phase dominates because of heightened Ge indiffusion while a higher  $\rho_c$  occurs when Au areas predominate. The present results suggest an alternate explanation: the Ni<sub>3</sub>GeAs and NiAs phases may actually be separated from the GaAs by a very thin layer (not yet observed) of interface Ge and are thus associated with a low  $\phi_B$  ( $\sim 0.25$ – $0.4$  eV); the Au phase is associated with a high  $\phi_B$  ( $\sim 0.7$ – $0.9$  eV). Consequently, with this model the minimum  $\rho_c$  for an alloyed AuGeNi ohmic contact is obtained when the interface area of phases associated with a low  $\phi_B$  is greatest.

The large variation in  $\phi_B$ , from  $\sim 0.25$  to  $0.9$  eV, for the different model interface structures suggests that low  $\rho_c$  nonalloyed ohmic contacts that use Au, Ge, and Ni can be made to  $n$ -GaAs ( $N_D > 5 \times 10^{18}$  cm<sup>-3</sup>) if interface composition is controlled to minimize  $\phi_B$ . For example, a properly fabricated Au-NiAs-Ge(As) contact should have a low  $\phi_B$  over the entire contact area.<sup>18</sup> The  $\sim 0.65$  eV range in  $\phi_B$  also has implications for GaAs Schottky barrier models in that  $\phi_B$  at GaAs interfaces cannot be assumed *a priori* to be restricted to values of  $\sim 0.7$ – $0.9$  eV.

This work was supported by Air Force Office of Scientific Research contract No. F49620-85-C-0120.

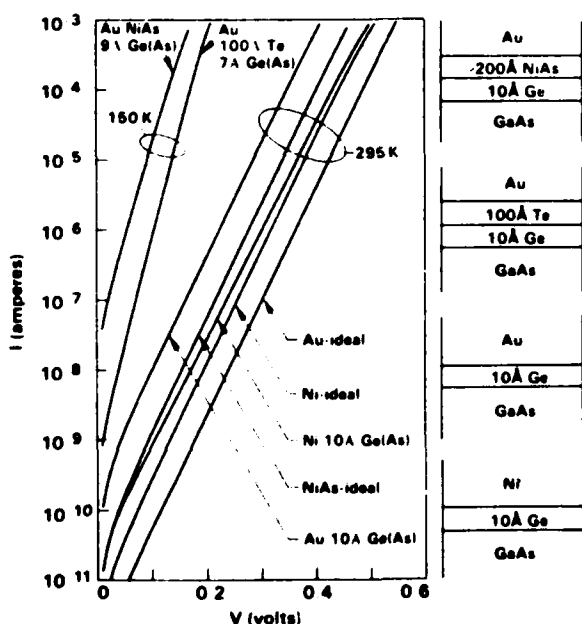


FIG. 3. Representative  $I$ - $V$  data for a selection of contacts to GaAs that have a variety of structures (contact area =  $5.07 \times 10^{-4}$  cm<sup>2</sup>). Multilayered contact structures are shown schematically on right.

<sup>1</sup>N. Braslau, J. B. Gunn, and J. L. Staples, *Solid State Electron.* **10**, 381 (1967).

<sup>2</sup>G. Y. Robinson, *Solid State Electron.* **18**, 331 (1975).

<sup>3</sup>M. Ogawa, *J. Appl. Phys.* **51**, 406 (1980).

<sup>4</sup>T. S. Kuan, P. E. Batson, T. N. Jackson, H. Rupprecht, and E. L. Wilkie, *J. Appl. Phys.* **54**, 6952 (1983).

<sup>5</sup>A recent review with an extensive bibliography is C. J. Palmström and D. V. Morgan, in *Gallium Arsenide*, edited by M. J. Howes and D. V. Morgan (Wiley, Chichester, 1985), Chap. 6.

<sup>6</sup>F. A. Kroger, G. Diemer, and H. A. Klasens, *Phys. Rev.* **103**, 279 (1956).

<sup>7</sup>C. Y. Chang, Y. K. Fang, and S. M. Sze, *Solid State Electron.* **14**, 541 (1971).

<sup>8</sup>W. G. Spitzer and C. A. Mead, *J. Appl. Phys.* **34**, 3061 (1963).

<sup>9</sup>J. R. Waldrop, *J. Vac. Sci. Technol.* **B2**, 445 (1984), *Appl. Phys. Lett.* **44**, 1002 (1984).

<sup>10</sup>H. Brugger, F. Schäfer, and G. Abstreiter, *Phys. Rev. Lett.* **52**, 141 (1984).

<sup>11</sup>P. Chiaradia, A. D. Katnani, H. W. Sang, Jr., and R. S. Bauer, *Phys. Rev. Lett.* **52**, 1246 (1984).

<sup>12</sup>E. A. Kraut, R. W. Grant, J. R. Waldrop, and S. P. Kowalczyk, *Phys. Rev. B* **28**, 1965 (1983).

<sup>13</sup>R. W. Grant, J. R. Waldrop, S. P. Kowalczyk, and E. A. Kraut, *J. Vac. Sci. Technol.* **19**, 477 (1981).

<sup>14</sup>E. H. Rhoderick, *Metal-Semiconductor Contacts* (Clarendon, Oxford, 1977).

<sup>15</sup>The large increase in band bending following metal depositions directly on the Ge layers (Fig. 1) in addition to the high and low  $\phi_B$  values measured by  $I$ - $V$  on similarly prepared Ge layers (Table I) rules out tunneling as a dominant conduction mechanism for our samples.

<sup>16</sup>This  $\phi_B$  for Ni-ideal is somewhat higher than the  $0.77$  eV reported in Ref. 9, which indicates that ideal Ni contacts appear not to have a unique  $\phi_B$ .

<sup>17</sup>J. R. Waldrop, *Appl. Phys. Lett.* **47**, 1301 (1985).

<sup>18</sup>For another nonalloyed GaAs ohmic contact approach, which uses a Au Schottky barrier to a thick Ge-GaAs heterojunction, see R. Stall, C. E. C. Wood, K. Board, and L. F. Eastman, *Electron Lett.* **15**, 800 (1979). In this case  $\phi_B$  (Au-Ge) =  $\sim 0.5$  eV.

END

7-87

DTIC